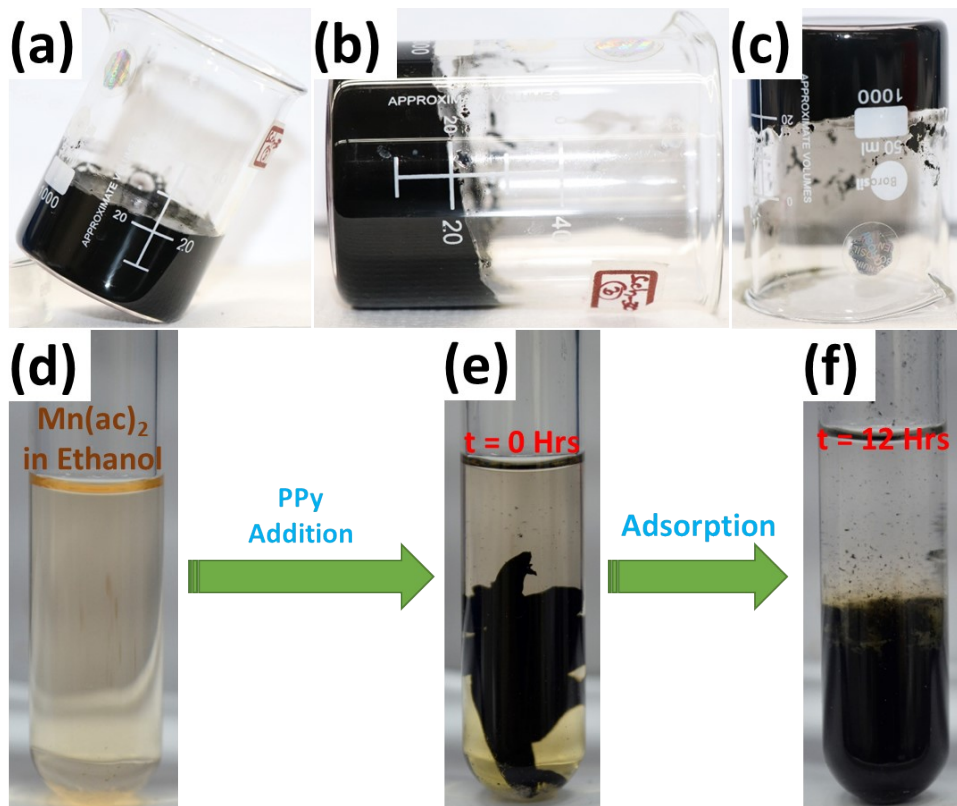


## Electronic Supplementary Information

### A polypyrrole derived nitrogen doped porous carbon support for atomically dispersed Mn electrocatalyst for oxygen reduction reaction

Sanjit Kumar Parida,<sup>\*a</sup> Tulasi Barik,<sup>b</sup> Hrudananda Jena<sup>\*a</sup>



**Fig. S1** Photographs of PPy hydrogel (a)-(c) and Mn(ac)<sub>2</sub> loaded PPy at different time intervals (d)-(g).

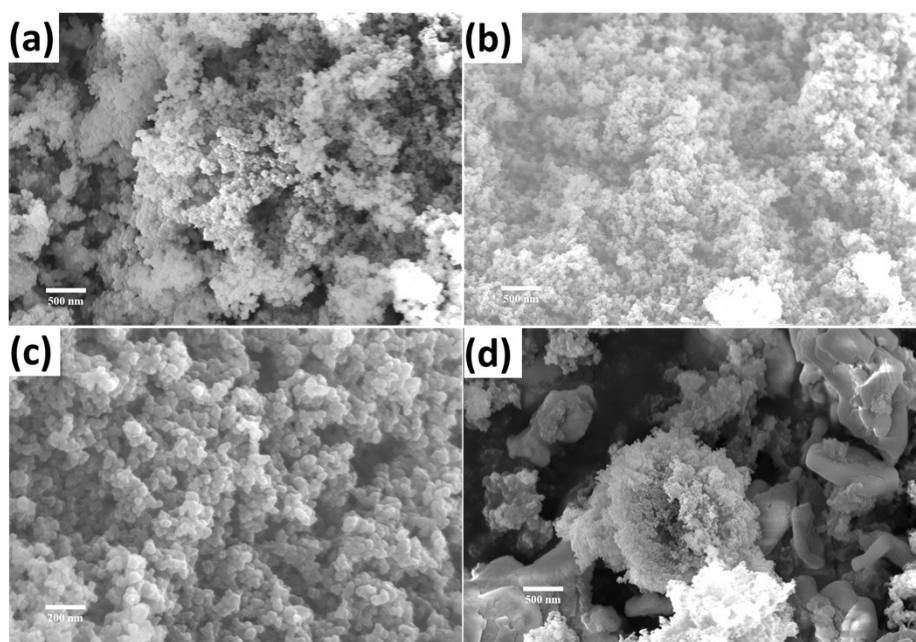


**Fig. S2** FESEM images of (a) 0Mn@PPy (b, c) 0.01Mn@PPy (d) 0.1Mn@PPy.

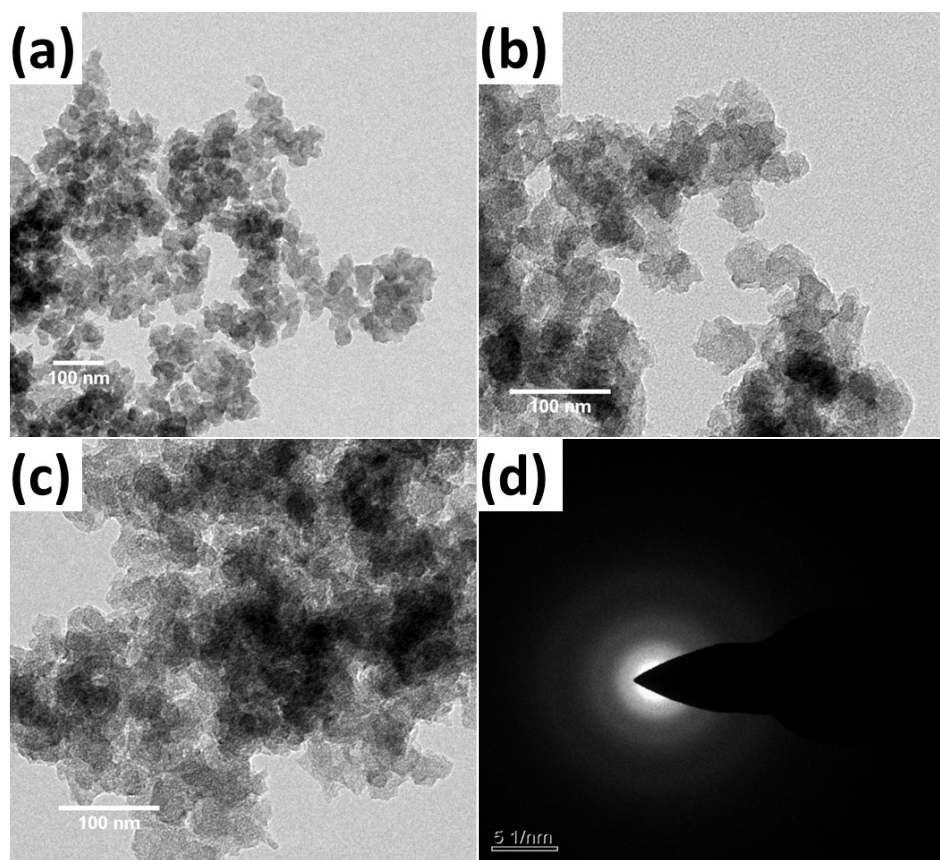


**Fig. S3** Representative TEM images of (a) 0Mn-N-C, (b) 0.01Mn-N-C, (c) 0.1Mn-N-C and (d) SAED pattern of 0.01Mn-N-C.

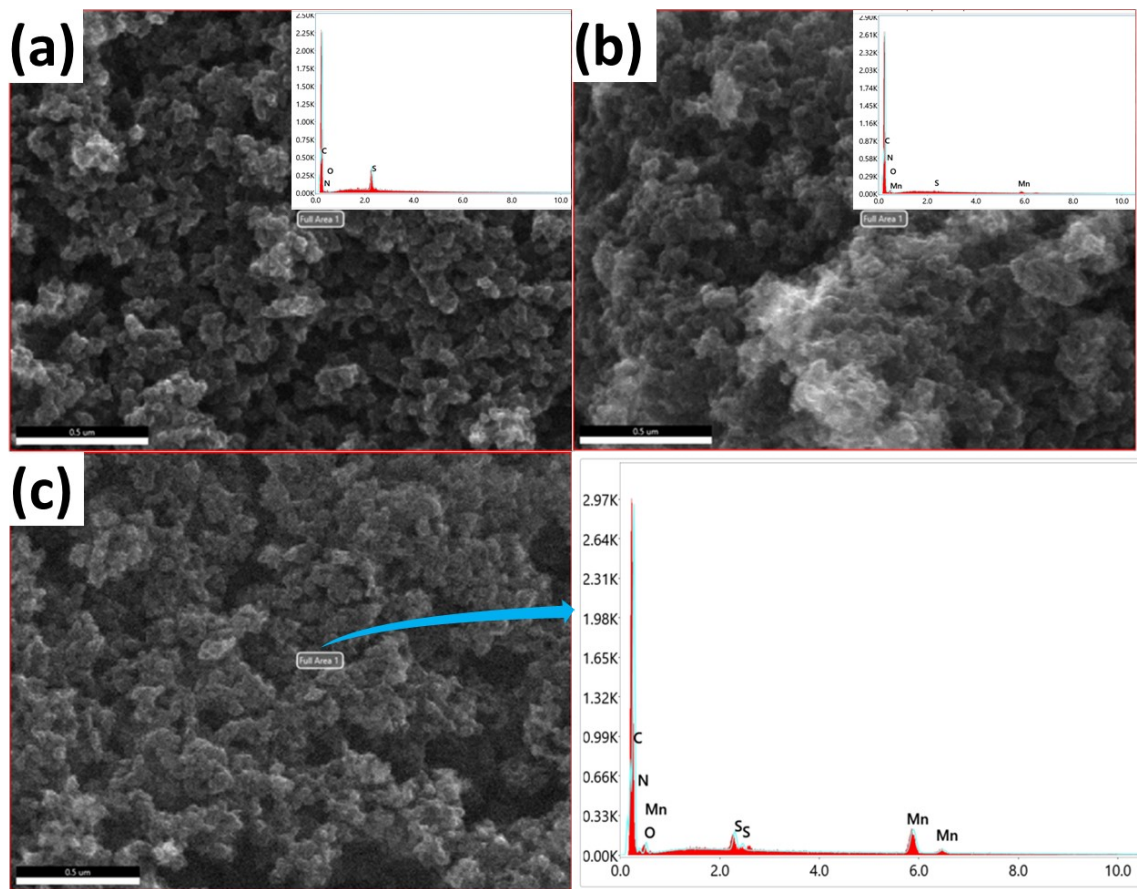


**Fig. S4** SEM image with corresponding EDX pattern of (a) 0Mn-N-C, (b) 0.1Mn-N-C and (c) 0.01Mn-N-C.

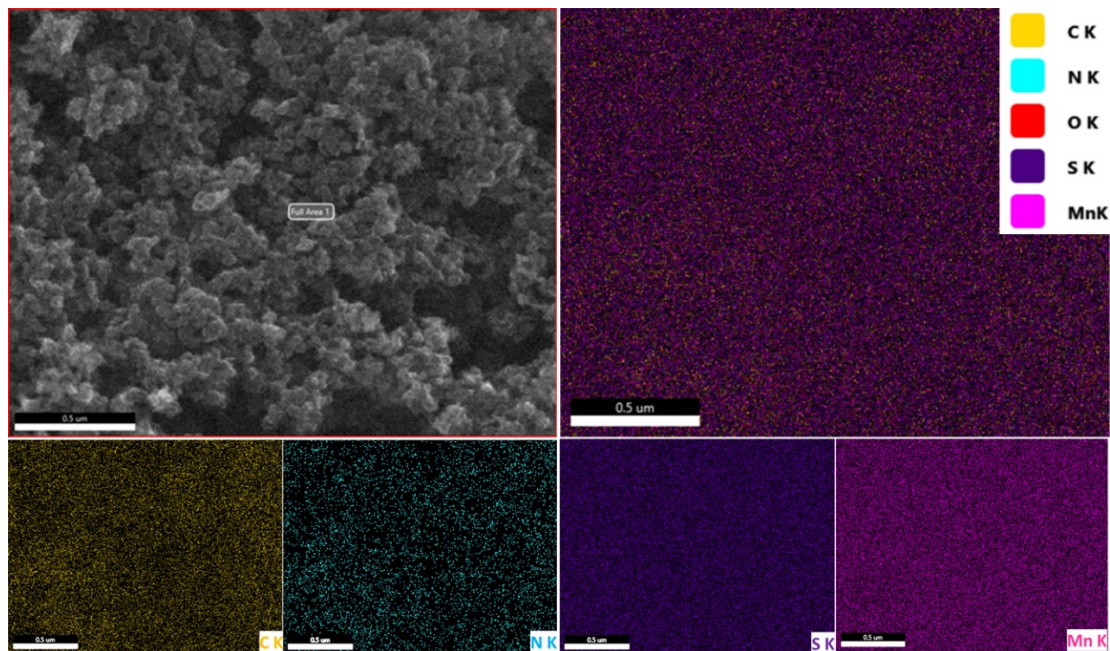


**Fig. S5** SEM image with EDX elemental mapping of 0.01Mn-N-C.

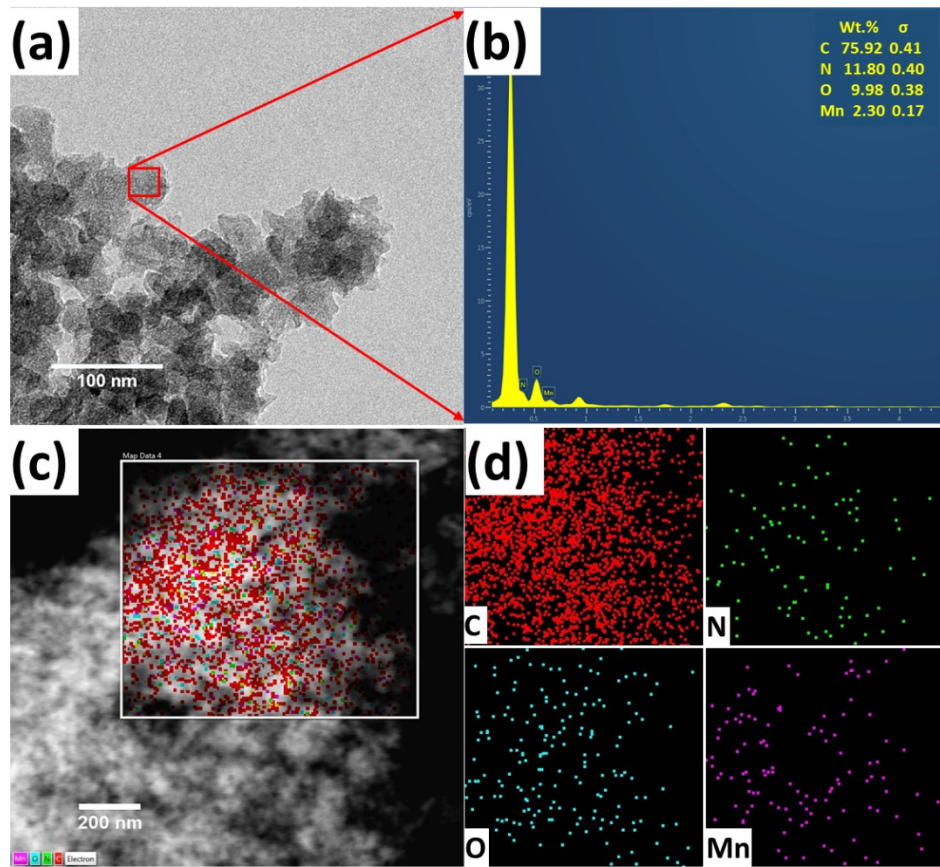


**Fig. S6** (a) STEM image, (b) EDS pattern and (c, d) EDX elemental mapping of 0.01Mn-N-C.

**Table S1. BET surface area and pore size of the catalysts.**

Catalyst	SA <sub>BET</sub> (m <sup>2</sup> /g)	SA <sub>Micro</sub> (m <sup>2</sup> /g)	V <sub>Micro</sub> (cc/g)	V <sub>Meso</sub> (cc/g)	V <sub>Total</sub> (cc/g)
0Mn-N-C	411.485	168.369	0.073	0.390	1.487
0.01Mn-N-C	492.621	49.466	0.024	0.432	1.590
0.1Mn-N-C	209.104	11.023	0.006	0.203	0.2639

**Table S2. Elemental composition of catalysts as obtained from XPS and ICP-OES.**

Catalyst	At. % Composition (XPS)					Wt.% (ICP-OES)
	C	N	O	S	Mn	
0Mn-N-C	86.5	9.1	3.5	0.9	0.0	0.00
0.01Mn-N-C	80.2	8.8	7.6	1.6	1.8	2.66
0.1Mn-N-C	86.3	6.2	6.1	0.3	0.8	1.90

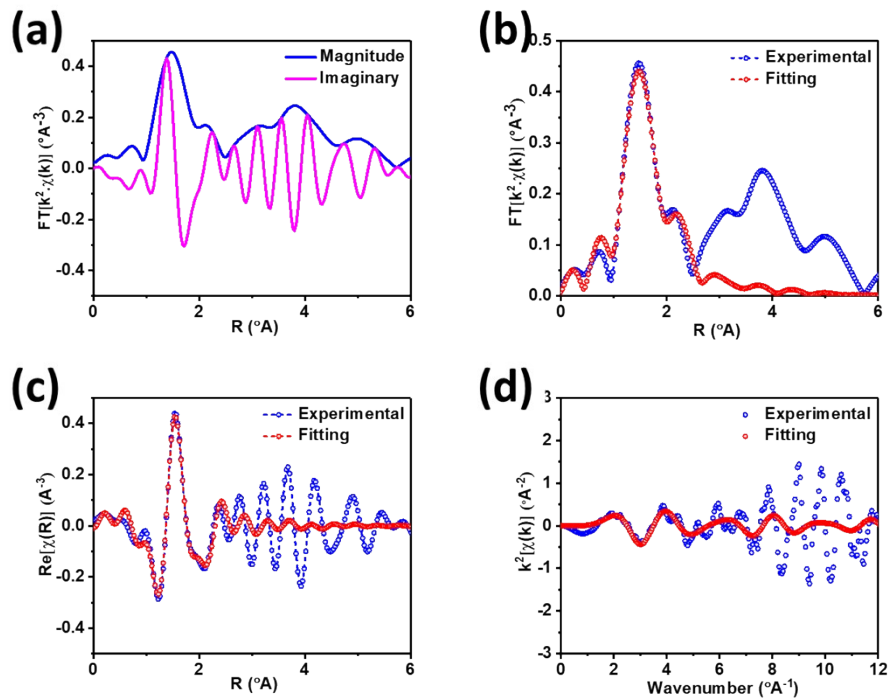


**Fig. S7** (a) The magnitude and imaginary part of the FT-EXAFS of 0.01Mn-N-C. The experimental and fitting curves of FT-EXAFS of 0.01Mn-N-C in (b, c) R-space and (d) k-space.

**Table S3. Fitting parameters of Mn K-edge EXAFS for 0.01Mn-N-C.**

Path	N	R ( $\text{\AA}$ )	$\sigma^2$	$\Delta E_0$ (eV)	R-factor
Mn-N	4	$2.067 \pm 0.025$	$0.0009 \pm 0.0029$	$1.286 \pm 1.848$	0.091

N: Coordination number; R: the distance between absorber and backscatter atoms (equals to the bond length of Mn-N);  $\sigma^2$ : the Debye-Waller factor value;  $\Delta E_0$ : the inner potential correction to account for the difference in the inner potential between the sample and the reference compound.

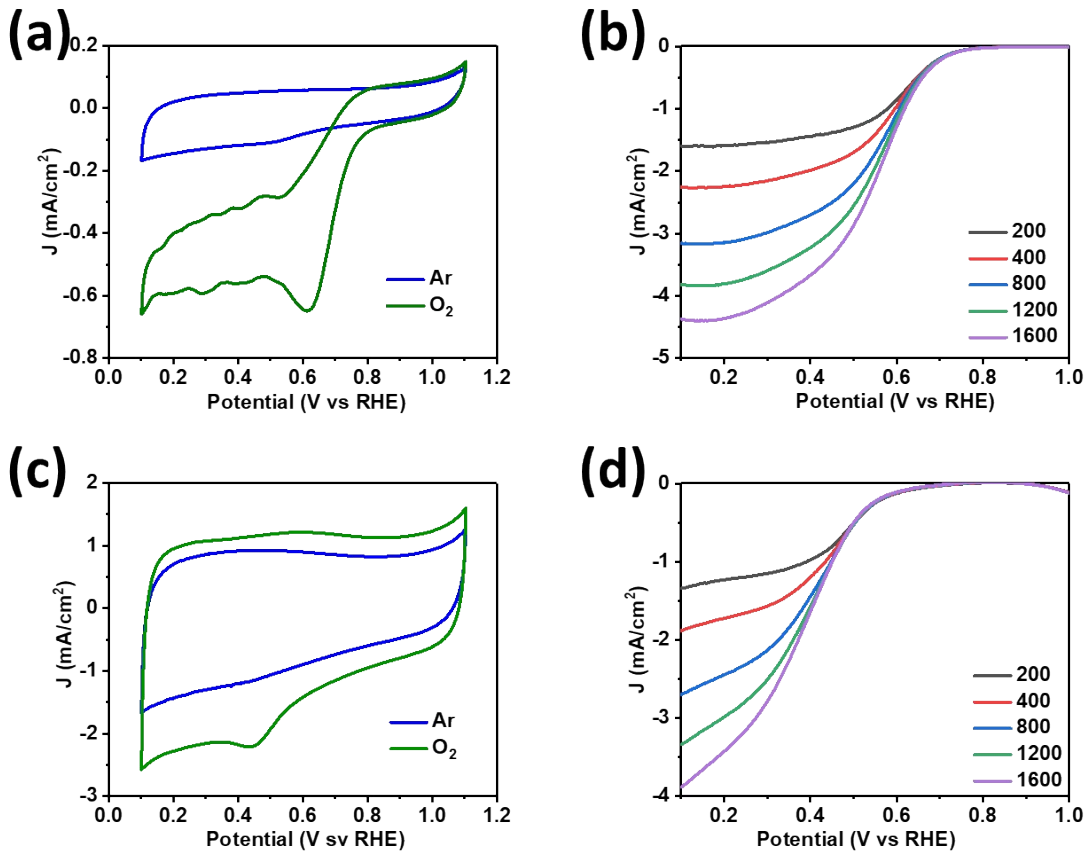


**Fig. S8** (a) CV, (b) LSV of 0.01Mn-N-C and (c) CV, (d) LSV of 0Mn-N-C in 0.5M H<sub>2</sub>SO<sub>4</sub>.

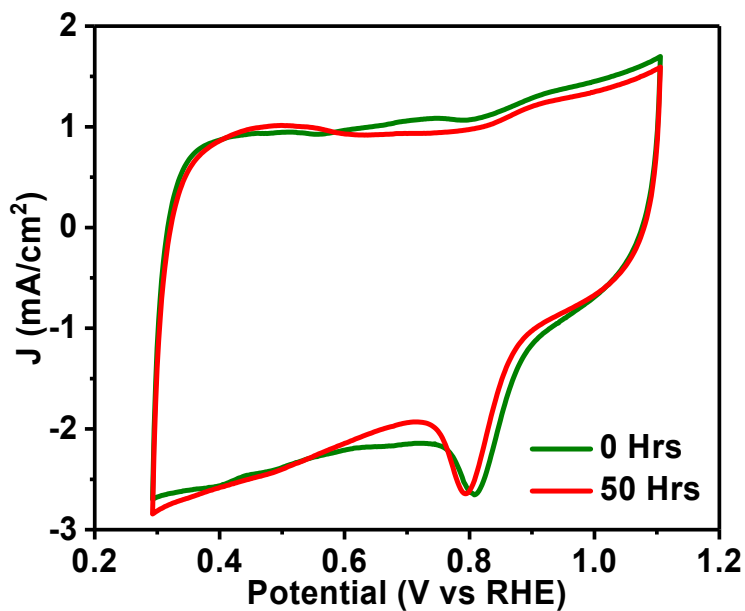


**Fig. S9** CV of 0.01Mn-N-C after chronoamperometric test at 0.7V vs RHE at 1600 RPM in O<sub>2</sub> saturated 0.1M KOH.

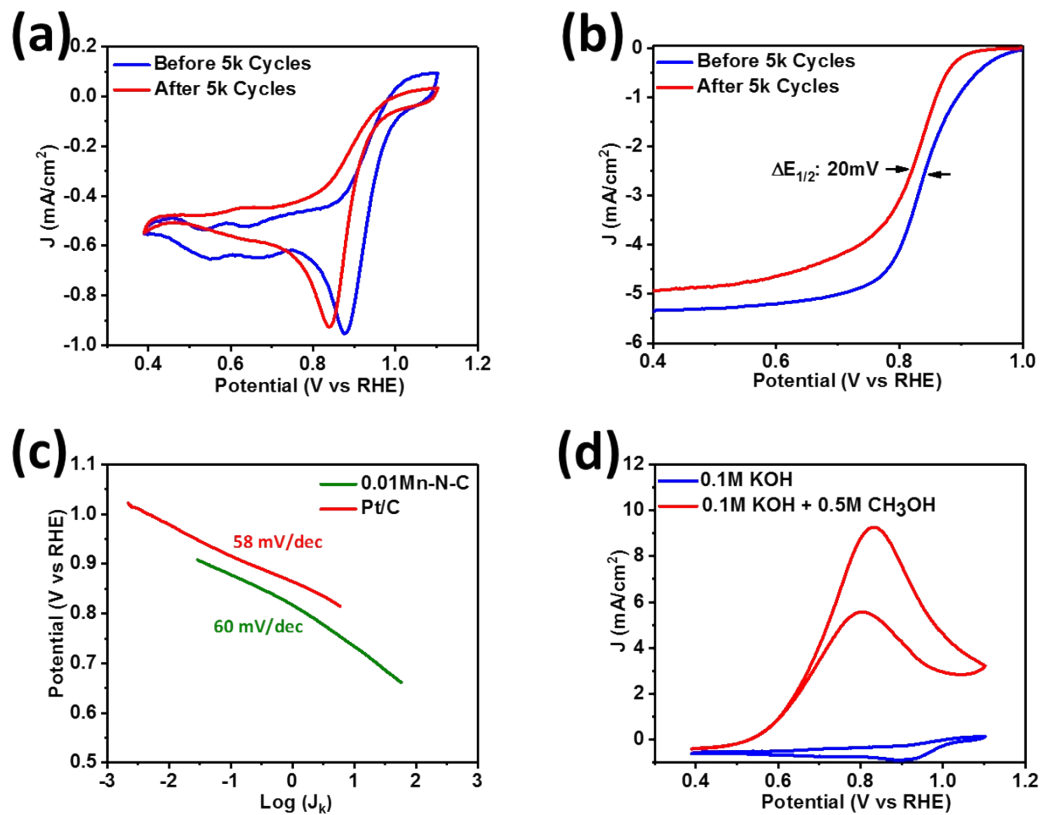


**Fig. S10** (a) CV and (b) LSV of Pt/C before and after accelerated durability test (ADT). (c) Tafel slopes of 0.01Mn-N-C and Pt/C after ADT. (d) CV of Pt/C in  $\text{O}_2$  saturated 0.1M KOH and 0.1M KOH+0.5M CH<sub>3</sub>OH in methanol tolerance test.

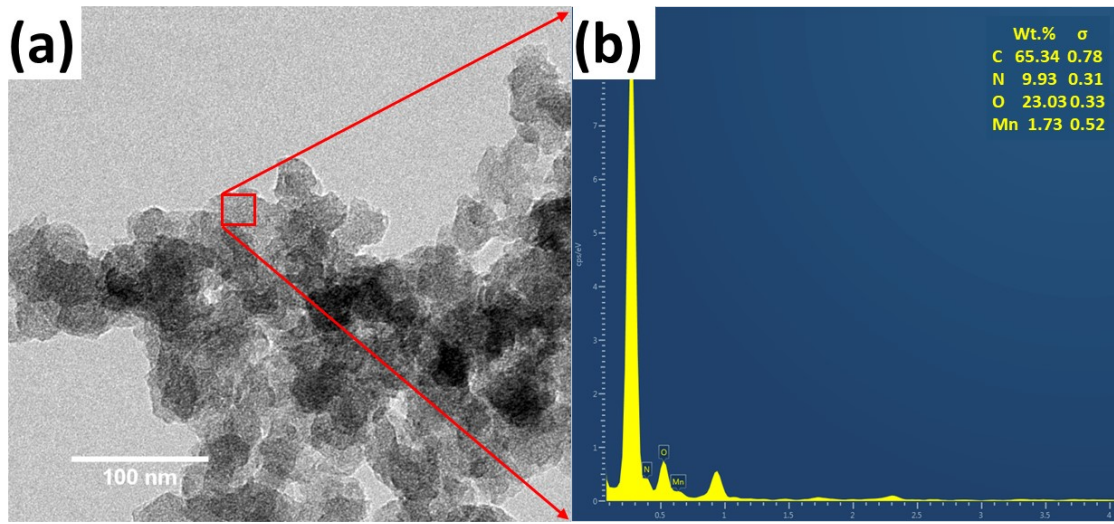


**Fig. S11** (a) STEM image and (b) corresponding EDX pattern of 0.01Mn-N-C after ADT.

**Table S3.** Review of ORR activity of Mn single-atom catalysts in 0.1M KOH reported in recent literature.

Catalyst	Mn Content	Loading ( $\mu\text{g}/\text{cm}^2$ )	$E_{\text{on}}$ (V vs RHE)	$E_{1/2}$ (V vs RHE)	Ref.
<b>0.01Mn-N-C</b>	<b>2.66 wt%</b>	<b>400</b>	<b>0.91</b>	<b>0.82</b>	<b>This work</b>
MnNC	7.88 wt%	500	0.97	0.86	[1]
Mn-N-C-OAc-10-Second	0.36 at%	800	-	0.94	[2]
Mn-NAHPC-900	0.76 wt%	263	0.96	0.86	[3]
Mn-SA	1.8 wt%	200	0.99	0.87	[4]
Mn-N-C900	0.27 at%	600	0.98	0.88	[5]
MnSAC	1.85 wt%	102	1.04	0.915	[6]
MnN <sub>4</sub> @rGO	-	250	0.91	0.86	[7]
Mn@NG	0.5 wt%	300	0.95	0.82	[8]
MnNPC-900	0.39 wt%	400	0.97	0.84	[9]
f-MnNC/CNT-170	0.67 at%	260	0.91	0.83	[10]

**References:**

- [1] ACS Sustainable Chem. Eng. 2022, 10, 1, 224–233.
- [2] J. Mater. Chem. A, 2022, 10, 2826-2834.
- [3] Int. J. Hydrog. Energy 46 (1), 2021, 543-554.
- [4] ACS Sustainable Chem. Eng. 2020, 8, 427–434.
- [5] ACS Sustainable Chem. Eng. 2020, 8, 25, 9367–9376.
- [6] Nano Lett. 2020, 20, 5443-5450.
- [7] Inorg. Chem. Commun. 2020, 112, 107700.
- [8] Applied Catalysis B: Environmental 257 (2019) 117930.
- [9] Small 2019, 15, 1804524.
- [10] Nanoscale 2019, 11, 15900-15906.